

Conformational States of Cytochrome P450cam Revealed by Trapping of Synthetic Molecular Wires

Anna-Maria A. Hays¹, Alexander R. Dunn², Richard Chiu², Harry B. Gray²
C. David Stout¹ and David B. Goodin^{1*}

¹Department of Molecular Biology, The Scripps Research Institute, 10550 North Torrey Pines Road, La Jolla, CA 92037 USA

²Beckman Institute, California Institute of Technology, Pasadena, CA 91125, USA

Members of the ubiquitous cytochrome P450 family catalyze a vast range of biologically significant reactions in mammals, plants, fungi, and bacteria. Some P450s display a remarkable promiscuity in substrate recognition, while others are very specific with respect to substrate binding or regio and stereo-selective catalysis. Recent results have suggested that conformational flexibility in the substrate access channel of many P450s may play an important role in controlling these effects. Here, we report the X-ray crystal structures at 1.8 Å and 1.5 Å of cytochrome P450cam complexed with two synthetic molecular wires, D-4-Ad and D-8-Ad, consisting of a dansyl fluorophore linked to an adamantyl substrate analog *via* an α,ω -diaminoalkane chain of varying length. Both wires bind with the adamantyl moiety in similar positions at the camphor-binding site. However, each wire induces a distinct conformational response in the protein that differs from the camphor-bound structure. The changes involve significant movements of the F, G, and I helices, allowing the substrate access channel to adapt to the variable length of the probe. Wire-induced opening of the substrate channel also alters the I helix bulge and Thr252 at the active site with binding of water that has been proposed to assist in peroxy bond cleavage. The structures suggest that the coupling of substrate-induced conformational changes to active-site residues may be different in P450cam and recently described mammalian P450 structures. The wire-induced changes may be representative of the conformational intermediates that must exist transiently during substrate entry and product egress, providing a view of how substrates enter the deeply buried active site. They also support observed examples of conformational plasticity that are believed to be responsible for the promiscuity of drug metabolizing P450s. Observation of such large changes in P450cam suggests that substrate channel plasticity is a general property inherent to all P450 structures.

© 2004 Elsevier Ltd. All rights reserved.

Keywords: molecular wires; sensitizer linked substrates; cytochrome P450; substrate recognition; X-ray crystallography

*Corresponding author

Introduction

Molecular recognition and catalysis involve varying degrees of protein structural plasticity and movement.¹ Identification of examples of

such movement and their characterization will significantly aid our understanding of how proteins adopt either specific or promiscuous binding behavior. The ubiquitous cytochrome P450 family exhibits these features, catalyzing a vast range of biologically significant reactions in mammals, plants, fungi, and bacteria.² Examples of P450s are well known to detoxify xenobiotics, catabolize substrates as a carbon source, or synthesize biologically active compounds such as steroids, prostaglandins, and other metabolites of arachidonic acid.^{2–4} Elucidating the structural and biochemical mechanisms governing P450 functional diversity is

Present addresses: A.-M. A. Hays, Ambrx Inc., 10410 Science Center Dr., San Diego, CA 92121, USA; A. R. Dunn, Department of Biochemistry, Stanford University, Stanford, CA 94305, USA.

Abbreviation used: PEG, polyethylene glycol.

E-mail address of the corresponding author: dbg@scripps.edu

crucial due to the potential application of these enzymes in many areas of biotechnology, bio-transformation, bio-sensing, and pharmacology.^{5–7} Interestingly, P450s can exhibit a remarkable flexibility at the substrate-binding site. This permits significant substrate motility within the substrate-binding cavity, and can result in a mixture of products.⁸ Some P450s are even able to accommodate multiple ligands simultaneously.^{9–16} Because different members of the P450 family utilize such a diverse group of substrates, and because an individual P450 can display remarkable substrate promiscuity, it has been proposed that many P450s possess a significant degree of structural plasticity.^{2,17,18}

Despite the low level of sequence identity among P450s,^{2,3,19} recent crystallographic structures of mammalian P450s^{15,16,20,21} demonstrate that the overall structural fold of eukaryotic membrane-bound P450s is conserved and clearly resembles that of soluble bacterial P450s.^{19,22} Consequently, the well-characterized camphor-metabolizing cytochrome P450cam remains a useful model system for P450 structure and function.² The structure of P450cam from *Pseudomonas putida* consists of an asymmetrical triangular fold of 12 α -helices and five antiparallel β -sheets which deeply buries the thiol-coordinated heme in the hydrophobic core of the protein.^{2,23,24} The substrate-binding site is enclosed within the core of the protein on the distal side of the heme. Recognition of camphor by P450cam is governed by a hydrogen bond between the carbonyl group of camphor and the hydroxyl group of Tyr96, along with steric/hydrophobic interactions between the substrate and aromatic side-chains lining the binding site.^{23,24} P450cam is also able to bind numerous other ligands, including derivatives of camphor, styrene, and adamantane.^{17,25–32} Raag *et al.*²⁹ observed significant rearrangements of aromatic side-chains in the substrate-binding region of P450cam upon binding of an inhibitor more than twice the size of camphor.^{2,29} Studies of P450cam utilizing photoacoustic calorimetry identified large enthalpic and volumetric changes upon substrate release, strongly suggesting significant structural reorganization of the enzyme.^{33,34}

Further experimental and computational analyses provide evidence that P450cam controls substrate entry and product egress by protein fluctuations and ligand-dependent molecular associations.^{35–37} These studies with P450cam,^{36–38} and with P450BM3 and P450eryF³⁹ CYP51⁴⁰ and CYP154C1,⁴¹ suggest that significant motion of the substrate recognition regions is necessary for substrate binding, and that these regions must adjust their overall shape to accommodate the substrate.³ Finally, recent crystal structures of P450cam complexed with synthetic sensitizer-linked substrates (molecular wires), consisting of a substrate analog linked to a redox active [Ru(bpy)₃]²⁺ sensitizer *via* a covalent tether,^{42,43} directly revealed an altered conformational state in which the active

site is forced open by the wire. These probes bind to P450cam with high affinity and reveal a channel approximately 22 Å deep and 11 Å wide, leading from the protein surface to the deeply buried active site above the heme.⁴⁴

Here, we present crystal structures of P450cam complexed with two new wires, D-4-Ad and D-8-Ad (Figure 1), which incorporate a dansyl fluorophore linked to an adamantyl group *via* an α,ω -diaminoalkane chain varying in length. The variation in length of the hydrocarbon tether, either four or eight carbon atoms (D-4-Ad and D-8-Ad, respectively), dramatically changes the binding affinity (D-4-Ad $K_d = 0.83 \mu\text{M}$ and D-8-Ad $K_d \approx 0.02 \mu\text{M}$), although both exhibit higher affinity than the natural substrate camphor ($K_d = 1.6 \mu\text{M}$).^{25,45} The structures described here show that binding of these two wires induces a range of protein conformational changes that are distinct from those induced by camphor or previously studied wires. They demonstrate that the high complementarity between the wire and the protein is primarily due to conformational flexibility of the enzyme. Detailed analysis of the structures allows the identification of key protein–ligand interactions that contribute to binding affinity and specificity, and thus provide insight into the differing affinities of each of the probes for the enzyme.

The D-4-Ad and D-8-Ad bound structures represent intermediate conformations between the extreme open form, found with the bulky [Ru^{II}(bpy)₃]²⁺ sensitizer, and the closed camphor-bound form of P450cam. We propose that this range of active site conformations mimics the conformational conversions that exist transiently in solution during substrate entry and product egress. In addition, these intermediate conformations provide evidence for the complementary nature and pliability of the P450cam active site in response to the introduction of a substrate. Detailed comparisons of these intermediate states demonstrate that specific features of the protein architecture mediate the structural plasticity exhibited by this enzyme family. Finally, we observe that the opening of the substrate access channel in response to wire binding induces changes at the active site that are

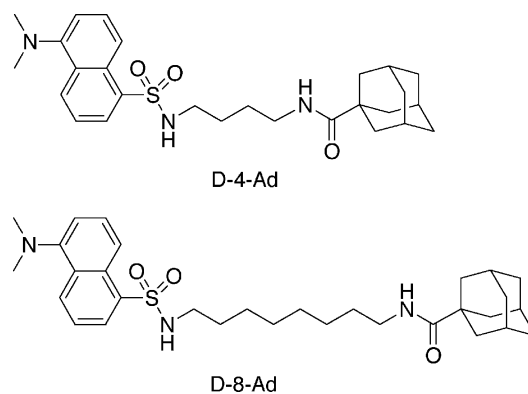


Figure 1. Structures of the synthetic molecular wires used here.

similar to those that are induced upon O₂ binding⁴⁶ and have been implicated in proton delivery upon cleavage of the peroxy bond.⁴⁷

Results

Crystal structures of P450cam with bound D-4-Ad and D-8-Ad were solved at 1.8 and 1.5 Å resolution, respectively, by molecular replacement utilizing the camphor-bound P450cam structure as an initial model (Table 1). Electron density for both wires is clear, particularly in the region near the adamantyl groups in the active site on the distal side of the heme (Figure 2B). The aliphatic tethers are held between the helix-rich domain and the mostly anti-parallel β-sheet domain, with the dansyl groups placed either within the protein channel or at the protein surface, depending on the length of the linker (Figure 2). Although both wires bind at similar positions within the protein, they induce protein conformations that are distinct from each other and from the camphor-bound structure. These global conformational changes propagate from the periphery into the protein active site, revealing the remarkable flexibility of the P450cam substrate-binding region.

Recognition of D-4-Ad and D-8-Ad by cytochrome P450cam

The adamantyl moiety makes hydrophobic interactions with several substrate-binding site residues that are similar to those observed between camphor and P450cam. A key interaction is also formed between the carbonyl group of the adamantyl and the Tyr96 side-chain. This hydrogen bond is virtually identical in length with that observed with camphor (2.7 Å), and participates in a

hydrogen-bonding network with Tyr96 and Thr101 that is similar to that found in the camphor-bound structure (Figure 2B). The adamantyl groups of each probe are located 4.5 Å from the heme (based on closest approach), very similar to the distance observed for camphor (4.3 Å). Binding of D-4-Ad to P450cam induces shifts in the positions of Tyr96 and Phe193. The side-chain of Tyr96 rotates somewhat to allow hydrogen bonding to the carbonyl group of the adamantyl. In addition, Phe193 reorients to accommodate the linker and dansyl group. D-8-Ad binding induces very similar changes at Tyr96, but the perturbation at Phe193 is not as large, requiring smaller shifts in the surrounding hydrophobic residues. As observed with camphor, numerous hydrophobic interactions are formed between the adamantyl and Thr252, Val295, Asp297, and Val396. In addition, the protein interactions with the adamantyl of D-4-Ad resemble those seen with camphor somewhat more closely than for D-8-Ad due to additional van der Waals contact with Thr101.

The aliphatic linkers of D-4-Ad and D-8-Ad assume similar positions as they thread through the region above the substrate-binding site. In addition, each of the structures displays similar side-chain rotamers for the hydrophobic side-chains lining the substrate access channel. Additional hydrophobic interactions are formed between the linker of D-8-Ad and Phe87, Val247, and Ile395 that are not observed for the shorter linker of D-4-Ad. Thus, the numerous hydrophobic interactions between the wires and the enzyme can be expected to contribute significantly to the stabilization of the respective protein conformations.

The largest differences in the binding of D-4-Ad and D-8-Ad to P450cam are seen at the dansyl group (Figure 2C and D). The sulfonamide of the

Table 1. Crystallographic statistics

Diffraction data	D-8-Ad	D-4-Ad
PDB code	1RE9	1RF9
Space group	<i>P</i> 2 ₁ 2 ₁ 2 ₁	<i>P</i> 2 ₁ 2 ₁ 2 ₁
Unit cell (Å)	<i>a</i> = 64.57, <i>b</i> = 75.94, <i>c</i> = 92.40	<i>a</i> = 65.13, <i>b</i> = 75.11, <i>c</i> = 93.17
Resolution (Å)	20–1.45 (1.51–1.45) ^{a,b}	20–1.8 (1.86–1.8) ^a
No. reflections (total/unique)	214,985/72,960	122,587/38,960
Multiplicity	2.97	3.15
Completeness (%)	94.1 (92.2) ^a	90.7 (88.6) ^a
<i>R</i> _{sym}	0.077 (0.60) ^a	0.063 (0.34) ^a
<i>I</i> / σ (<i>I</i>)	12.4 (1.3) ^a	17.9 (2.0) ^a
Wilson <i>B</i> factor (Å ²)	12.6	19.83
Refinement statistics	CNS/ShellX	CNS
<i>R</i> _{factor} ^c (<i>R</i> _{free} ^d)	15.8 (21.5)	19.6 (22.7)
No. protein atoms, avg. <i>B</i> (Å ²)	3200, 16.98	3200, 23.43
No. water molecules, avg. <i>B</i> (Å ²)	274, 26.78	237, 30.67
No. heme atoms, avg. <i>B</i> (Å ²)	43, 7.85	43, 10.87
No. ligand atoms, avg. <i>B</i> (Å ²)	38, 37.06	34, 39.62
rms bond lengths (Å), angles (deg.) ^e	0.010, 0.03	0.006, 1.275

^a Outer shell statistics.

^b Due to anisotropy in the diffraction, reflections in the shell 1.51–1.45 Å with $|F| > 2.0 \sigma(F)$ were included in the refinement; $\langle I \rangle / \langle \sigma(I) \rangle$ in the shell 1.58–1.51 Å is 1.9 (*R*_{sym} = 0.459).

^c $R = \sum ||F_{obs}| - |F_{calc}|| / \sum |F_{obs}|$ for all reflections (no σ cutoff).

^d Free *R* calculated using 4.8% as test set.

^e rms deviations from ideal bond and angle restraints.

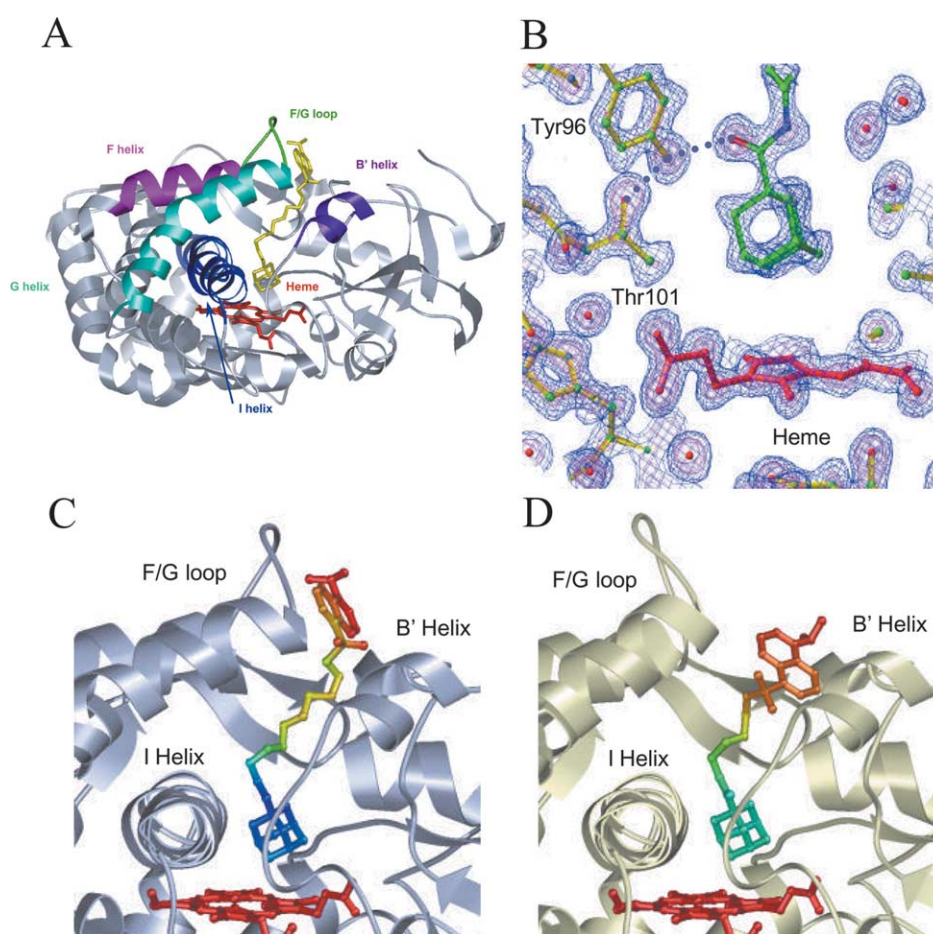


Figure 2. Structures of D-8-Ad and D-4-Ad probes bound to P450cam. Overall structural fold (with D-8-Ad bound) is shown in A, highlighting elements that are involved in substrate recognition, binding, and catalysis. The σ_A -weighted $2F_o - F_c$ electron density map for D-8-Ad is shown in B contoured at 1.5σ and superimposed on the final model. The hydrogen bond between Tyr96 and the carbonyl group of D-8-Ad is indicated. In C and D, the D-8-Ad and D-4-Ad probes are colored by increasing temperature factor from blue to red.

dansyl group in D-4-Ad is sequestered between the side-chains of Phe193 on the G helix and Phe87 of the B' helix, and forms a hydrogen bond with a solvent molecule (Wat4223). The naphthyl and dimethylamino groups form extensive hydrophobic interactions with side-chains of the B' helix (Tyr29, Ile88, Ala92, and Ile395). The dansyl in this position is sterically compatible with the protein only after the substantial retraction of the F/G helix-loop region (Figure 3). This includes residues 173–185 on the F helix, residues 192–214 on the G helix, and residues 186–191 in the F/G loop. Conversely, the extended aliphatic linker of D-8-Ad allows the fluorophore to lie at the solvent-accessible surface. As a result, the F/G region can adopt a more closed conformation with D-8-Ad than for D-4-Ad. The D-8-Ad sulfonamide group is not solvated; rather, van der Waals contacts are formed with side-chains originating from the B' helix. The dansyl fluorophore of D-8-Ad, located at the surface of the protein, was observed in different conformations in each of two independently solved structures, while the protein structure near this group was the same in both structures. In the 2.2 Å resolution

structure,⁴⁵ the naphthyl portion of the dansyl interacts with Pro89 of the B' helix, whereas it interacts with Pro187 of the F/G loop in the 1.5 Å resolution structure.

The above observations are consistent with the degree of disorder seen in the wires as indicated by the observed B values. The adamantyl segments of the wires, deeply buried in the protein cleft, are highly ordered. As depicted in Figure 2C and D, the average B values for the adamantyl groups are 23.94 \AA^2 and 13.71 \AA^2 for D-4-Ad and D-8-Ad, respectively, similar to the average overall B values of the protein (23.34 \AA^2 and 16.9 \AA^2 for D-4-Ad and D-8-Ad, respectively). In contrast, the average B values of the dansyl groups are 51.58 \AA^2 and 55.29 \AA^2 for D-4-Ad and D-8-Ad, respectively. This suggests that the interactions between the dansyl group and the surrounding protein are weak, consistent with considerable static and/or dynamic disorder in the outer segment of the bound wire. In addition, there is a smooth transition from low to high B value as the length of the linker of either probe traverses from the interior to the surface of the protein.

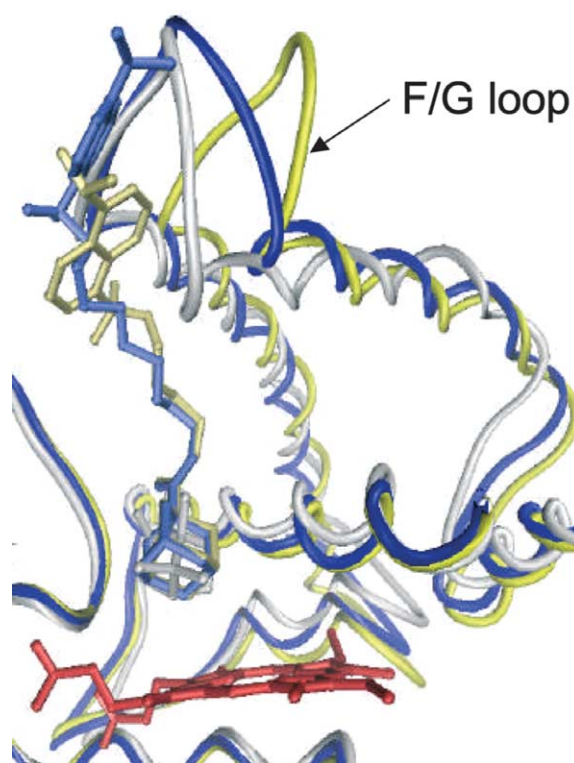


Figure 3. Superposition of the structures of P450cam bound to camphor (white) pdb code 2CPP,²⁴ D-8-Ad (blue), and D-4-Ad (yellow).

F/G domain changes associated with SLS binding

Upon D-4-Ad or D-8-Ad binding, the F/G region retracts from the heme-containing protein core by rotating about an axis nearly parallel with the I helix (Figure 4). This hinge motion opens a 22 Å deep channel from the protein surface to the buried active site above the heme (Figure 5). This general movement is observed with both wires, but is more pronounced in the D-4-Ad structure (14° rotation for D-4-Ad as compared to the 11° rotation for D-8-Ad as measured by DynDom.^{48,49}).

The retraction of the F/G region in response to the binding of the wires is accompanied by displacement of Pro187 (F/G loop) from its position in the closed camphor-bound form by 6.5 Å and 3.4 Å for D-4-Ad and D-8-Ad, respectively. Two distinct movements are observed as one progresses from the fully closed (camphor) conformation, through the partially open (D-8-Ad) form, to the fully open (D-4-Ad) state. The first change, from closed to intermediate, involves primarily a shift in position of the F helix along with part of the F/G loop. In the second transition, from intermediate to fully open, the F helix remains in the intermediate conformation, while the G helix undergoes a retraction across the I helix. Several residues within the F/G region accompany the domain movement by undergoing large changes in ϕ/ψ of $>20^\circ$. In addition, residues 299–231 of the 5-1 and 5-2

β -sheets undergo significant backbone conformational changes upon opening of the substrate access channel. In comparison, Pro157 and Ala167 of the E helix along with Thr185 of the F helix undergo substantial ϕ/ψ rearrangements in the D-8-Ad structure as the F helix moves backward. As the G helix maintains a position similar to the closed camphor-bound form, residues of the F/G loop undergo a considerable twisting motion.

Changes in the interaction of the F/G domain with the remainder of the protein

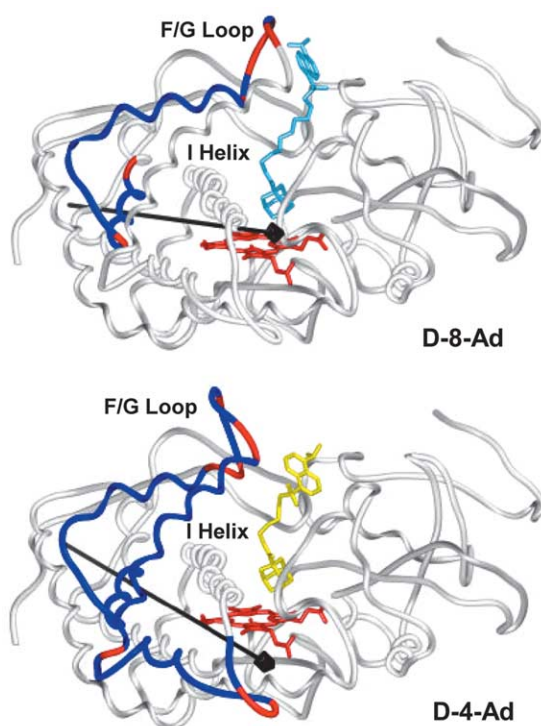
As shown in Figure 2A, the I helix spans the width of the molecule, and lies directly between the heme and the F/G helices as they fold over the substrate-binding site. Not surprisingly, the retraction of the F/G region observed upon binding of the wires alters its interactions with the I helix. In the closed, camphor-bound structure, a salt-bridge and hydrogen bonding network exist between the F and I helices that includes the side-chains of Asp251 and Asn255 of the I helix and Lys178, Asp182, Thr185, Arg186 of the F helix (Figure 6). In the D-4-Ad complex (Figure 6C), these residues readjust to form contacts with the neighboring E helix, β -sheet 4-1, and newly introduced solvent molecules. However, in the D-8-Ad complex (Figure 6B), the diminished movement of the F helix permits the hydrogen bond between Asp251 and Thr185 to be maintained. Additional interactions between the F and I helix are disrupted by the upward and back movement of the F helix, resulting in the reorientation of F helix residues toward nearby E helix residues or solvent molecules.

A second key salt-bridge in the camphor-bound structure is observed between Asp97 of the B' helix and Lys197 of the G helix. This interaction is completely disrupted upon the retraction of the G helix away from the B' helix to accommodate the D-4-Ad wire. In the D-4-Ad bound state, the Lys197 side-chain readjusts to form a hydrogen bond with the side-chain of Glu198, while the side-chain of Asp97 is not able to re-establish any interactions with nearby residues or solvent molecules. In contrast, the more limited movement of the F helix in the D-8-Ad structure allows the salt-bridge between the G and B' helices to be maintained.

Also noteworthy is a significant shift of the E helix in both the D-4-Ad and D-8-Ad structures. Two E helix residues, Ile160 and Phe163, which form a hydrophobic pocket for the I helix Leu250 side-chain in the camphor-bound structure, shift approximately 1.6 Å along the helical axis upon binding of the wires and necessitate the rearrangement of inter and intra-residue interactions. Consequently, this region is highly sensitive to the retraction of the F helix.

Protein B factors

Most, but not all, of the regions undergoing significant movement also display significantly higher average B values in comparison to the



Compared to Camphor-bound P450	Domain Movement	Residues (> 20° phi/psi rotation)	Rotation (deg)
D8-Ad	E-helix (160 – 171) F-helix (174 – 182)	E-helix P157, A167 F-helix T185 F/G-loop P187, D88, G189, M191	11.3
D-4-Ad	E, F, G, H-helices (159 – 225) 5-1, 5-2 sheet (226 – 233)	F helix T185, E3, M184 F/G-loop Asp188 G helix T192, F193, Q13 N29, G230, R31	13.9

Figure 4. Decomposition analysis of domain movements induced by D-8-Ad or D-4-Ad binding to P450cam. The specific domains undergoing significant movement upon probe binding are colored in blue, whereas hinge residues modulating these movements by undergoing large ϕ/ψ changes are colored in red. The black arrows depict the rotational axis of the F/G region as it retracts from the heme-containing protein core by rotational motion (14° rotation for D-4-Ad as compared to the 11° rotation for D-8-Ad) as measured by DynDom.⁴⁸

protein core (Figure 7). In the D-4-Ad structure, the F and G helices along with the F/G loop have substantially higher B values (33.0, 41.9, and 60.7 Å², respectively) compared with the overall average B value of the enzyme (18.8 Å²). In contrast, the average B value of the I helix, which also undergoes conformational change upon binding, is only 17.8 Å² for the D-4-Ad structure. Comparable values are obtained for the D-8-Ad structure with the exception that the G helix displays a lower average B value than the F helix (Figure 7).

Wire-induced changes in hydration of the substrate-binding channel

The conformational changes induced by wire binding to P450cam also provide increased solvent access within the occupied substrate access channel. The largest channel is induced by D-4-Ad binding, and in addition to the wire, nine solvent molecules are observed in the electron density map that were

not observed in the closed camphor-bound structure (Figure 5). Wat4010 and Wat4249 may stabilize the conformational change in the I helix by forming hydrogen bonds with both main-chain and side-chain atoms of I helix residues. Wat4031 mediates interaction between an amide nitrogen atom on D-4-Ad and the Asp251 side-chain. The remaining solvent molecules in the channel are positioned to replace hydrogen bonds that were disrupted during the opening of the channel. These new solvent molecules form bridging interactions between the I, F, and E helices, and mediate interactions between the I helix and β -sheets 4-1 and 4-2. One solvent peak, labeled Wat4223, is observed in the channel opening near the solvent-accessible surface, and is unusual, in that it makes no readily identifiable hydrogen bonds. This position is occupied by the main chain of Phe193 of the G helix in the closed camphor-bound structure.

The more constricted channel of the D-8-Ad bound structure is also significantly hydrated,

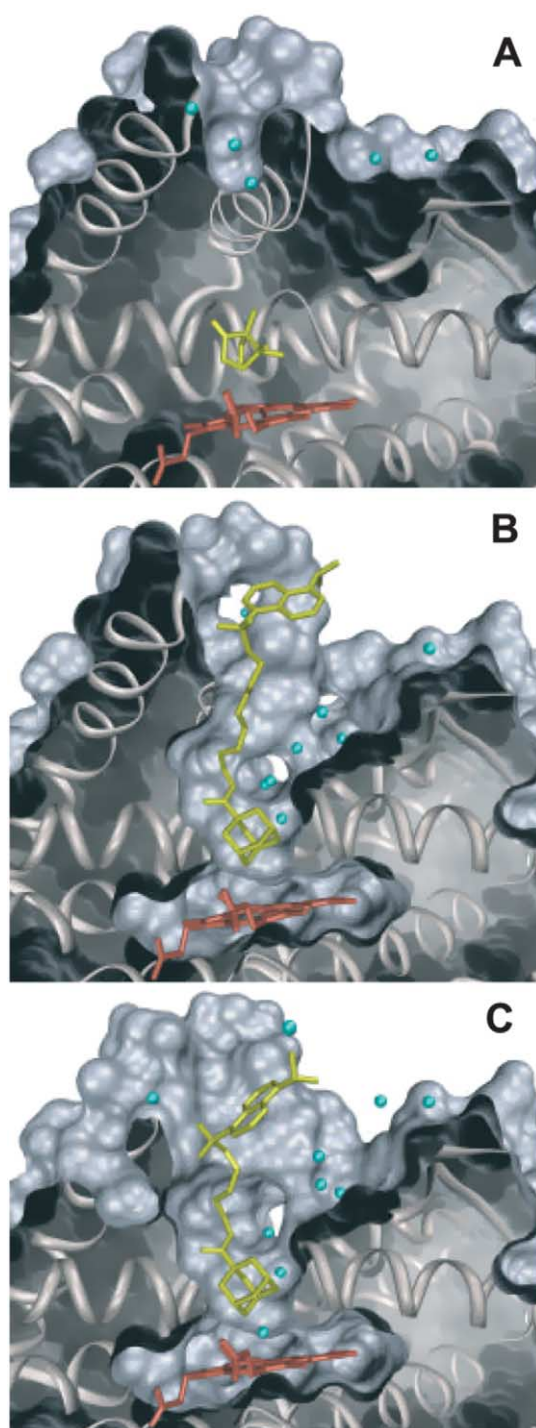


Figure 5. Cross-sections of the solvent-accessible surface for camphor-bound (A), D-8-Ad-bound (B), and D-4-Ad-bound P450cam (C). Positions of ordered solvent are shown in cyan.

with eight observed solvent peaks (Figure 5). Wat4156 interacts with residues of the F/G loop that have moved as the F helix recedes to accommodate D-8-Ad. The remaining solvent molecules are observed in positions that are roughly analogous to those seen in the D-4-Ad structure. Both structures also contain two highly

ordered solvent molecules that bridge a gap between the B' helix and the 1–4 β -sheet, as interactions between the two structural elements are disrupted by a small wire-induced readjustment of the B' helix. In both structures, approximately 20 highly ordered solvent molecules bind P450cam, hydrating newly exposed surfaces and bridging interactions disrupted upon wire binding.

Changes at the active site

Movements in the F/G helix induced by wire binding are observed to propagate to residues that serve catalytically important roles at the active site. In native P450cam, the I helix is broken into N and C-terminal halves by a central bulge (Figure 8). Thr252 is at the position of the helical bulge and forms hydrogen bonds with main-chain atoms exposed by disruption of the helix. This residue, along with the adjacent Asp251, have been long implicated in proton delivery during the cleavage of the peroxy bond in catalysis.^{2,46,47} In response to wire-induced movements of the F/G domain, the I helix bulge shifts and rotates to maintain packing interactions with Leu236 and Leu240 (Figure 9A). In both wire-bound structures, the α -helical hydrogen-bonding pattern is extended through residues Leu250, Asp251 and Thr252, resulting in a shift of the helix bulge toward the N terminus by three residues. This helical realignment is accompanied by large ϕ/ψ changes ($\Delta\phi=46.4^\circ$, $\Delta\psi=63.8^\circ$ for D-4-Ad, and $\Delta\phi=46.4^\circ$, $\Delta\psi=63.8^\circ$ for D-8-Ad). In addition, the shift in the helix bulge results in the release of carbonyl groups on Val247, Leu246, and Leu245 from canonical helical hydrogen bonds and the formation of new interactions with solvent (Figure 8). The change in the I helix bulge is essentially the same for the D-4-Ad and D-8-Ad bound forms. As a result of this shift, the positions of the functionally important Thr252 and Asp251 are significantly displaced upon opening of the substrate access channel. These changes are analogous to those induced by O₂ binding to ferrous P450cam,⁴⁶ including the binding of a water molecule, Wat47, that is analogous to the one proposed to participate in proton delivery to the bound O₂ (Figure 9B).

Effects on heme coordination

Camphor binding is known to alter the coordination of water to the heme at the active site of P450cam, and this change in coordination is believed to be a critical trigger in the activation of the enzyme.^{50,51} It is thus of interest that we observe a difference in heme coordination in the D-8-Ad and D-4-Ad bound forms. An ordered solvent peak, Wat4170, is observed at 2.5 Å from the heme iron in the D-4-Ad bound state, while no evidence of such a peak is seen in the D-8-Ad structure. As noted above, the position of the adamantyl group with respect to the heme is essentially identical in both structures, yet wire binding introduces a significant

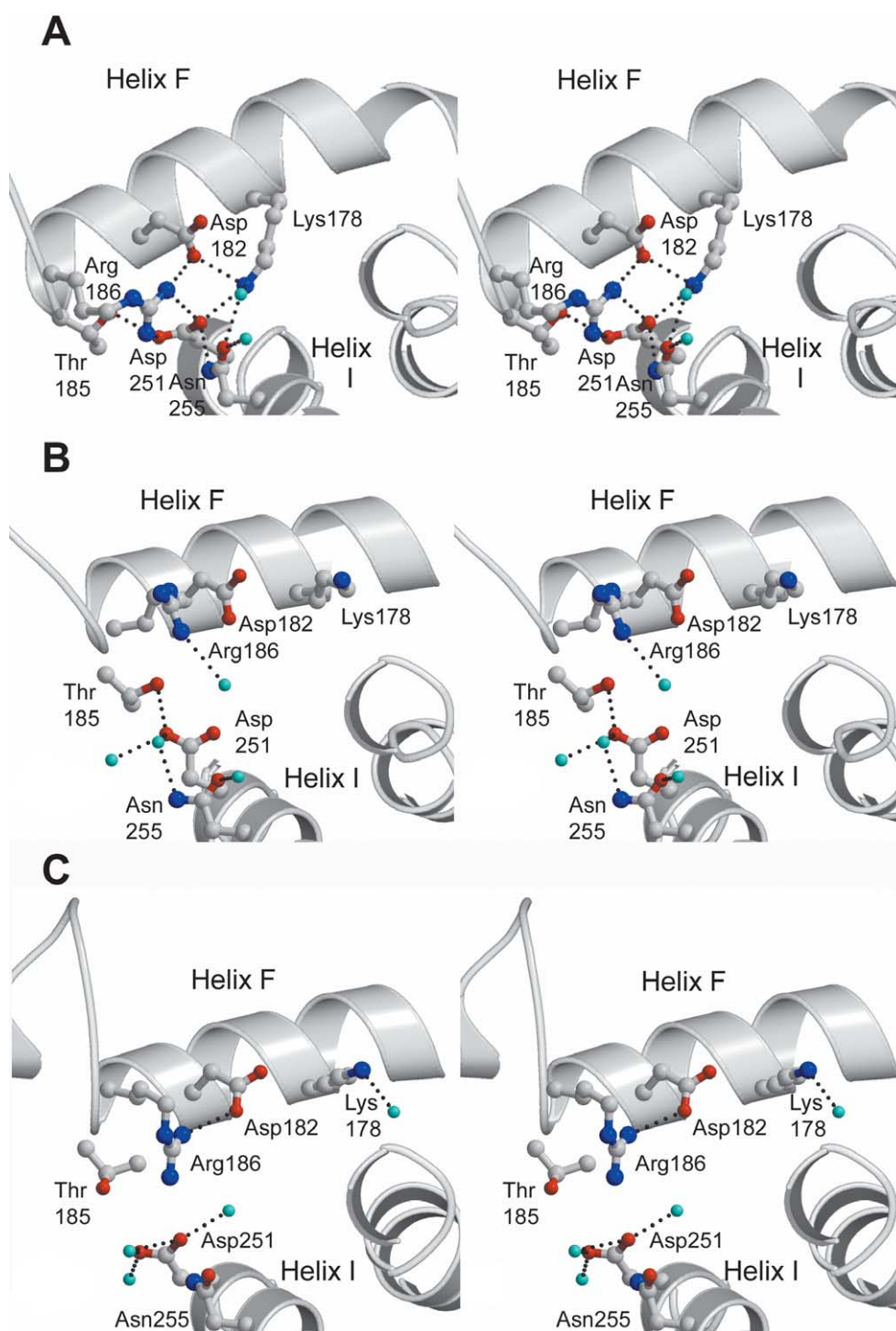


Figure 6. Stereoviews of salt-bridge and hydrogen-bonding interactions observed between the F and I helices for camphor-bound (A), D-8-Ad-bound (B), and D-4-Ad-bound P450cam (C).

change in the I helix. This shift brings the carbonyl group of Gly248 significantly closer to the heme (~ 4.2 Å) than is seen in the camphor-bound state (6.3 Å). However, this movement, and the changes observed in Asp251 and Thr252, are very similar for both D-8-Ad and D-4-Ad. Thus, the structural cause of the difference in water occupancy on the distal heme face between the two wire probes is not understood at present.

Discussion

The crystal structures of P450cam in complex with D-4-Ad and D-8-Ad provide insights into substrate-induced structural plasticity in P450s, and allow distinctions to be made between the response of P450cam to opening of the substrate channel and similar observations in other P450s. The retraction of the F and G helices and F/G loop from the

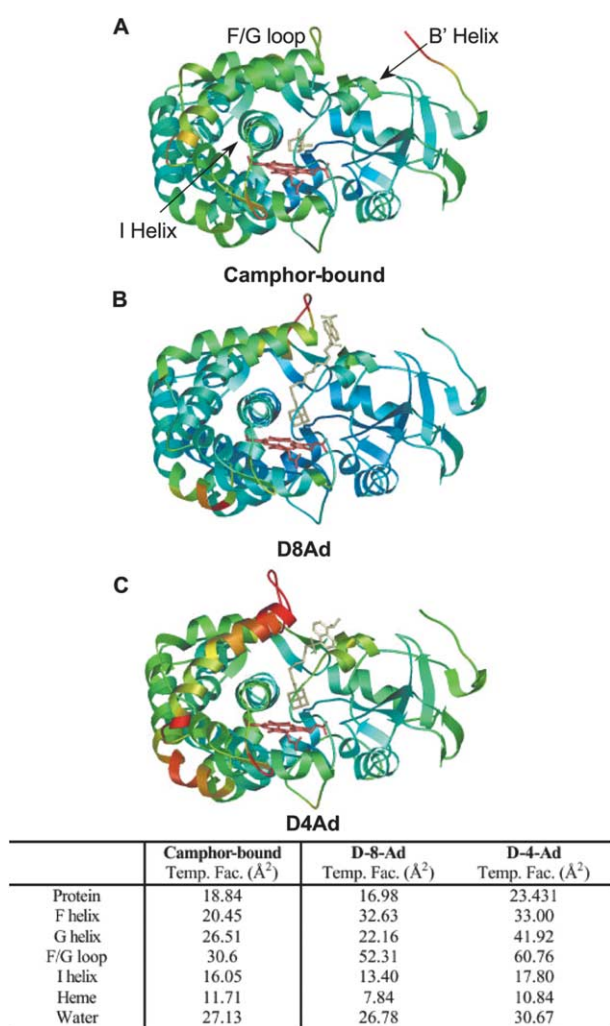


Figure 7. Variation in protein temperature factors. Ribbon diagrams of the protein models are shown for P450cam camphor-bound form (A), D-8-Ad (B), and D-4-Ad (C). Ribbons are colored blue to red by increasing protein *B* factors, while hemes are in red, irrespective of their temperature factors.

heme-containing protein core in response to wire binding has been observed previously.^{42–45,52} The additional conformations observed here arise from variation in the length of the linker between the dansyl group and the substrate analog of the wire probe. One of the important insights of this study is that shorter linkers are accommodated within the P450cam structure by the ability of the F/G helical region to adopt a range of alternate conformations rather than introducing changes at the more buried substrate end of the wire. This suggests that hydrogen bonding, shape complementarity, and hydrophobic interactions with the substrate analog portion of the wire dominate the binding energetics in these systems. To accommodate these changes, the protein responds with a remarkable degree of conformational plasticity that has been previously suggested from studies of substrate specificity.^{2,29–38} The active site of P450cam has even been observed

to accommodate a ferrocene derivative covalently linked to a cysteine residue,⁵² although the changes seen are quite different from those observed with the D-4-Ad and D-8-Ad wires. These new structures provide a wealth of direct information about the conformational alternatives available in the P450 active site. In addition, the variation in the surface exposure of the wire fluorophore suggests that these molecules may be useful probes of conformation and dynamics of the substrate-binding channel.

Structural plasticity of P450cam induced by wire binding

There appears to be a correlation between the extent of movement in the F/G loop region, binding affinity, and the degree of disorder in the structure in response to wire binding. For D-8-Ad, the linker is long enough to allow the dansyl group to extend to the solvent-accessible surface. As a result, the F/G loop can partially re-close to a conformation that is intermediate between the fully closed camphor bound form and that seen for wires containing more bulky Ru(bpy) sensitizers.^{42–44} For the shorter D-4-Ad, steric interactions between the dansyl group on the wire and the protein evoke a larger conformational change, as the F/G region is unable to re-close even to the extent seen for D-8-Ad. These observations are reflected in the *B* values of the F/G region. The larger temperature factors observed for D-4-Ad relative to D-8-Ad suggest a larger static disorder or dynamic movement in the more open D-4-Ad bound form. This, in turn, is consistent with the weaker affinity displayed by D-4-Ad. Similar correlations of increased protein temperature factors with diminished binding affinity were observed in complexes of P450cam with camphor analogs.^{23,29,50} Interestingly, the temperature factors in the F/G region of P450cam bound to a wire containing a [Ru^{II}(bpy)₃]²⁺ sensitizer were only slightly higher than those of the camphor-bound form despite the more open conformation of the F/G helix loop. This implies that the fully open conformation is stabilized by interactions between the bulky ruthenium complex and the surrounding protein. Previous comparisons of dynamic regions of a protein structure with observed temperature factors suggest that ligand-induced conformational changes reflect an intrinsic motion of the ligand-free protein.⁴⁸ Thus, conformational plasticity and dynamic motion of the F/G loop are likely to play important roles in the ability of P450 enzymes to adapt their binding sites to various substrates.

The coordinated movements in response to the opening of the F/G helix can be described by a shear mechanism that is common in proteins.^{53–55} The E, F, G, H, and I helices pack together by numerous interdigitated hydrophobic side-chains. Movement of the F/G segment induces a sliding motion in other regions that is a concatenation of many small readjustments of the hydrophobic

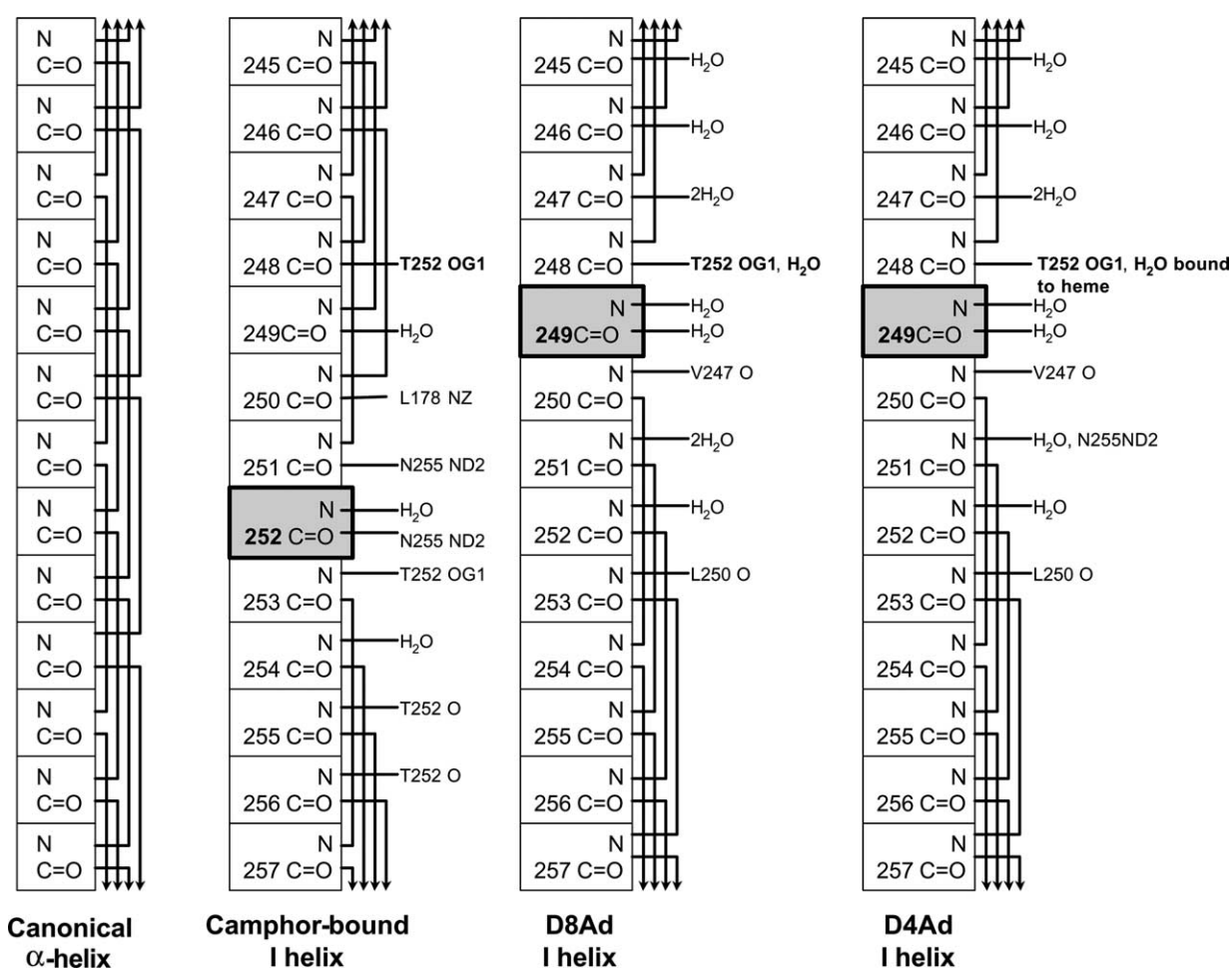


Figure 8. Comparison of observed hydrogen bonding patterns within the I helix showing the shift in the helical kink upon wire binding.

residues. These coordinated movements permit the densely packed hydrophobic interfaces to be maintained. Unlike many of the hydrophobic interactions, many salt-bridges and hydrogen bonds between the F and I helices as well as between the B' and G helices are disrupted in the more open D-4-Ad structure. On the other hand, only interactions between the F and I helices are broken in the more closed D-8-Ad conformation. These interactions have been proposed to act as a tether to prevent opening of the P450cam active site.^{34–38,56,57}

As illustrated by these structures, it is clear that substrate recognition in P450s is not solely determined by active-site residues near the binding site; substrate entry may be controlled significantly by protein motions of the substrate access channel. For example, a hydrophobic patch on the surface, including Phe193, has been proposed to control substrate entry and guide substrates to the active site.^{29,58} Conformational heterogeneity at a similar surface hydrophobic patch involving the B', F, and G helices is thought to play a critical role in substrate access and product egress.^{3,22,58} Substrate recognition in other P450s, including P450-BM3, CYP119, P450 2C5, and P450 2B4, is correlated with

large movements of the F/G region.^{16,21,59–61} These regions also possess higher temperature factors in P450terp, P450BM3, and P4502C5.^{20,56} Thus, many investigators have proposed an important role for protein dynamics and conformational heterogeneity in substrate recognition by P450s,^{33–35,57,58,62} and the conformations trapped by binding to D-4-Ad and D-8-Ad provide detailed suggestions of the specific intermediates that may be involved. In addition, the wire-induced changes in P450cam structure suggest that the promiscuity of substrate recognition due to F/G helix plasticity is an inherent, general property of the P450 fold.

Movement of the F/G domain influences the active site of P450cam

Coupling of the movements of the F/G loop with the shift in the I helix bulge may provide a mechanism for transmitting binding signals to the protein active site. The intimate interactions among the E, F, G, H, and I helices allow the I helix to respond to movements of the F/G region. The shift in the I helix bulge as the F/G helix retracts appears to be controlled by the protrusion of the I helix Leu250 side-chain into a hydrophobic pocket

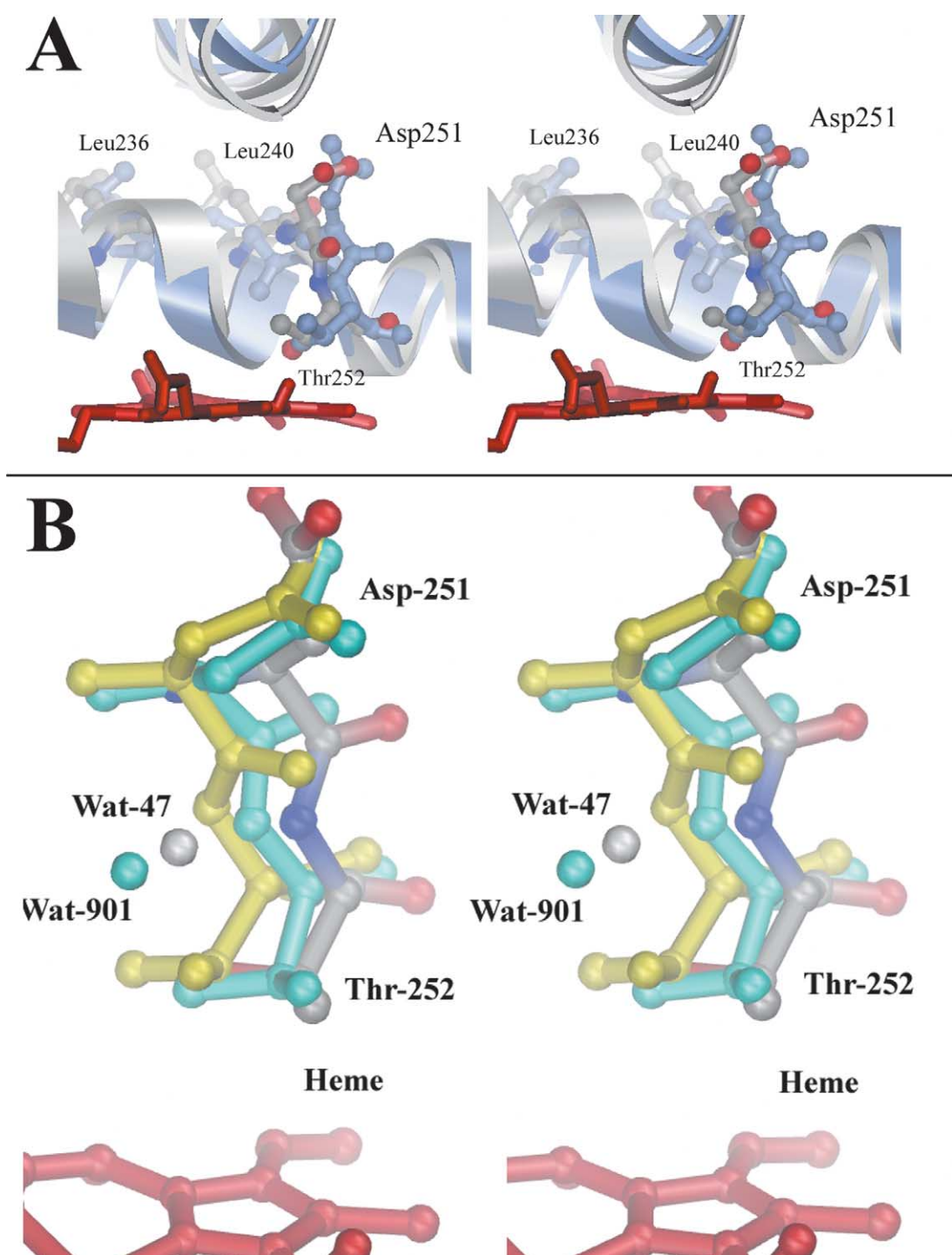


Figure 9. Stereoview showing changes in the active site residues of the I helix in response to wire binding. In A, the camphor-bound structure (pdb code 2CPP²⁴) is shown in atom colors, while the D-8-Ad-bound form is overlaid in blue. In B, the changes around Thr252 are shown in detail for camphor-bound ferric P450cam²⁴ (yellow), ferrous-O₂ P450cam (pdb code 1DZ8⁴⁶) (cyan), and the D-8-Ad-bound form (atom colors). No water is seen in the camphor-bound ferric P450cam, while Wat901 was observed in the ferrous-O₂ form. Wat47 is seen at a similar position in the D-8-Ad structure.

formed by Ile160 and Phe163 of the E helix. This protrusion changes upon movement of the E helix in response to the retraction of the F helix. In both the D-4-Ad and D-8-Ad structures, the E helix shifts approximately 1.6 Å along the helical axis, resulting in a shift in the side-chain of Ile160. This shift is

compatible with movement of the Leu250 side-chain as the I helix bulge shifts. Thus, it appears that the shift in the E helix, which is induced by wire binding, results in a shift in the helix I bulge as a result of a cog-and-groove-type interaction between these two helices. The I helix lies directly over the

heme distal face, and thus, the heme environment is likely affected by movements in the distal F/G helices. The highly conserved I helix contains Gly248, Asp251 and Thr252, which have been shown to be involved in proton delivery and stabilization of the dioxygen adduct at the heme active site.² The observed shift of the bulge in the I helix, directly above the heme, upon binding of either D-4-Ad or D-8-Ad, results in significant displacements of each of these important active-site residues. This suggests that the opening of the F/G region during substrate entry may trigger a molecular switch, brought about by the reorientation of the I helix that repositions these critical active site residues. Haines *et al.*⁶³ identified a similar movement of active-site residues induced by substrate binding to P450 BM3. P450 BM3 contains a residue analogous to Gly248, Ala264, which moves away from the active site upon substrate binding. In addition, a recent NMR study of P450cam⁶⁴ has demonstrated movements of the Thr252 side-chain upon binding of putidaredoxin. Most importantly, Schlichting *et al.* observed a clear reorientation of the Thr252 main-chain and side-chain upon O₂ binding to ferrous P450cam.⁴⁶ This movement allowed binding of a water molecule that was proposed to participate in proton delivery upon peroxy bond cleavage. These results suggest that O₂ or redox partner binding may trigger a functionally important structural switch allowing a critical step in dioxygen bond activation. As shown in Figure 9B, the retraction of the F/G helix across the I helix that is induced by wire binding results in changes at Thr252 and water binding that are very similar to these effects. Finally, recent structures of mammalian P450 2C5¹⁶ and 2B4^{21,62} indicate only small changes in the conformation of the analogous Thr residues, have little or no I helix bulge, and have (2B4) or do not have (2C5) the bound water analogous to Wat902 of ferrous O₂ or wire-bound P450cam. Thus, it is possible that changes in the active site may not be coupled substrate channel movements in the same way in P450cam and mammalian P450s.

Solvation changes associated with SLS binding to P450cam

The conformational changes associated with wire probe binding are accompanied by changes in protein solvation.^{44,65} A number of ordered solvent molecules are observed in newly formed cavities of the substrate channel, where they replace hydrogen bonds that were disrupted by binding of the wire probes. Notably, the positions of many of the solvent molecules observed in the channel are very similar in the D-4-Ad and D-8-Ad structures and in a previously characterized wire-bound structure.⁴⁴ Previous studies have shown that substrate analogs that do not optimally fit into the active-site channel of P450cam facilitate solvent access and disrupt the tight structural coupling for proton transfer.³² DiPrimo *et al.*⁶⁶ have identified as

many as 28 solvent molecules that are involved in P450cam substrate binding and catalysis. Changes in solvent access to the heme active site can be expected to have dramatic effects on heme reduction potential and electron transfer,^{65,67} and may thus provide another mechanism by which substrate-mediated conformational changes alter the functional behavior of P450s.

The difference in water coordination to the heme of P450cam in the D-8-Ad and D-4-Ad structures deserves comment. Substrate-free P450cam is low-spin due to coordination of a water molecule or hydroxyl group to the distal side of the heme.²³ This heme-bound water is displaced upon binding camphor, resulting in a shift in spin state and redox potential of the heme.⁵⁰ Adamantanone mimics the effects of camphor by displacing the heme-coordinated water, while smaller analogs, such as norcamphor, bind slightly further from the heme and thus do not displace the water ligand.⁵⁰ In the structures of D-8-Ad and D-4-Ad-bound forms of P450cam, the adamantyl substrate analogs are positioned at essentially the same location, and the distance of closest approach to the heme (4.5 Å) is very similar to that of camphor (4.3 Å). While the opening of the channel by the wire substrates induces changes in several active-site residues as discussed above, there is little difference at the active site between the D-8-Ad and D-4-Ad structures. Thus, it is puzzling that the distal heme water is fully displaced by D-8-Ad while it remains in the case of D-4-Ad. This may be the result of a very finely balanced set of structural and steric parameters that have not been fully revealed in the current structures.

Conclusions

The D-4-AD and D-8-Ad structures presented here provide insight into the conformational transitions that occur as substrates bind to the diverse class of P450 enzymes. The various conformational states that have been trapped by the bound synthetic wire probes of this study may thus provide a model for such intermediates. Transient opening of the putative substrate access channel is required for exchange of substrates and products. As a result of the plasticity of the structure surrounding the F/G helix, these wire-induced conformational changes produce a capacious cavity above the substrate-binding site of P450cam, providing a view of the ability of these enzymes to recognize a wide variety of substrates and ligands. The results also suggest that movements in the F/G region induced by the wire probes are coupled to changes at the active site similar in nature to those seen on O₂ or redox partner binding. The nature or existence of this coupling may be different in mammalian P450s. Overall, these results support the view that dynamic motions are an important feature of P450 substrate recognition, and that global architectural features that accommodate these structural changes are as finely tuned as the heme active site.

Material and Methods

Crystallization and data collection

Purification procedures for P450cam (C334A) were similar to those described by Dunn.⁴⁴ The complexes of P450cam bound to dansyloctyladamantane (D-8-Ad) and dansylbutyladamantane (D-4-Ad) were formed at a molar ratio of 1:1 at room temperature.⁴⁵ Diffraction-quality crystals were grown from 0.1 M citrate (pH 5.5), 200 mM KCl, 11–13% (w/v) polyethylene glycol (PEG; molecular mass 8000) using the hanging-drop, vapor-diffusion technique at 4 °C. The 1.5 Å and 1.8 Å datasets were collected at the Stanford Synchrotron Radiation Laboratory (SSRL) beamline 11-1 using an MAR image plate ($\lambda=1.00$ Å) from crystals soaked in mother liquor containing 30% ethylene glycol and flash-frozen in liquid nitrogen. Crystals were in the space group $P2_12_1$ with a single complex in the asymmetric unit (Matthews coefficient (V_M), 2.50; solvent content, 50%, v/v). Data were processed using DENZO and SCALEPACK.⁶⁸

Structure determination

Structures were solved by molecular replacement using the program AMoRE using the camphor-bound P450cam structure (PDB code 2CPP)²⁴ as an initial model from which all solvent molecules were removed. After initial rigid body refinement in CNS (Crystallography and NMR System),⁶⁹ iterative cycles of simulated annealing and B factor refinement using CNS and manual fitting using Xfit⁷⁰ were performed. The heme and wire probes were located in $F_o - F_c$ electron density difference maps and further refined by simulated annealing (CNS) and manual fitting (Xfit). For the 1.5 Å D-8-Ad dataset, CNS refinement was followed by refinement in SHELX-97.⁷¹ Distance, planarity, chiral volume, and anti-bumping restraints were applied from the onset of SHELX refinement, and after several rounds of refinement, anisotropic B factors were introduced. During the final round of refinement, Riding hydrogen atoms were added.

All models include residues 11–414 of P450cam, wire probe, heme, and water. The stereochemical parameters of the protein models were evaluated using PROCHECK,⁷² revealing that 98.8%, 100%, and 99.4% of the residues were in the most favored and generously favored regions of ϕ , ψ space for the 2.2 Å and 1.5 Å D-8-Ad and 1.8 Å D-4-Ad complexes, respectively. Refinement statistics for the 1.8 Å D-4-Ad and 1.5 Å D-8-Ad structures are shown in Table 1 (refinement statistics for the 2.2 Å D-8-Ad structure are shown for comparison purposes). Overall C^α RMSD for camphor-bound P450cam versus D-8-Ad is 0.86 Å, for camphor-bound P450cam versus D-4-Ad is 1.44 Å.

Structure analysis

The P450cam structures were superimposed using LSQKAB (CCP4) matching relatively invariant regions of the core protein (residues 59–75, 295–302, 315–326, 347–357). These residue ranges were determined iteratively by demanding that hydrophobic cores superimposed well without being influenced by changes of the F/G region. Conformational changes were analyzed using ϕ , ψ differences and domain movement analyzed using DynDom.⁴⁹ Figures were generated either by PMV (TSRI) or Ribbons.⁷³

Acknowledgements

The authors thank Dr Chris Putnam for discussion and critical reading of the manuscript. In addition, we thank Sophie Coon for providing support for PMV (TSRI). This work was supported by NSF (H.B.G.) and NIH grants GM41049 (to D.B.G.) and GM48495 (to D.B.G. and H.B.G.), and NIH NRSA postdoctoral fellowship GM20703-03 (to A.-M.A.H.). A.R.D. received support from the Fannie and John Hertz Foundation.

References

1. Hammes-Schiffer, S. (2002). Impact of enzyme motion on activity. *Biochemistry*, **41**, 13335–13343.
2. Ortiz de Montellano, P. R. (1995). (2 edit.) *Cytochrome P450: Structure, Function, and Biochemistry*. Plenum, New York.
3. Graham, S. E. & Peterson, J. A. (1999). How similar are P450s and what can their differences teach us? *Arch. Biochem. Biophys.* **369**, 24–29.
4. Anzenbacher, P. & Anzenbacherova, E. (2001). Cytochromes P450 and metabolism of xenobiotics. *Cell. Mol. Life Sci.* **58**, 737–747.
5. Wong, L.-L. (1998). Cytochrome P450 monooxygenases. *Curr. Opin. Chem. Biol.* **2**, 263–268.
6. Raucy, J. L. & Allen, S. W. (2001). Recent advances in P450 research. *Pharmacogenom. J.* **1**, 178–186.
7. Guengerich, F. P. (2002). Cytochrome P450 enzymes in the generation of commercial products. *Nature Rev. Drug Discov.* **1**, 359–366.
8. Ogury, K., Yamada, H. & Joshimura, H. (1994). Regiochemistry of cytochrome P450 isozymes. *Ann. Rev. Pharmacol. Toxicol.* **34**, 251–279.
9. Cupp-Vickery, J. A. R. & Hatziris, Z. (2000). Crystal structures of ligand complexes of P450eryF exhibiting homotropic cooperativity. *Proc. Natl Acad. Sci. USA*, **97**, 3050–3055.
10. Domanski, T. L., He, Y. A., Harlow, G. R. & Halpert, J. R. (2000). Dual role of human cytochrome P450 3A4 residue Phe-304 in substrate specificity and cooperativity. *J. Pharmacol. Expt. Ther.* **293**, 585–591.
11. Hosea, N. A., Miller, G. P. & Guengerich, R. P. (2000). Elucidation of distinct ligand binding sites for cytochrome P450 3A4. *Biochemistry*, **39**, 5929–5939.
12. Hutzler, J. M., Hauer, M. J. & Tracy, T. S. (2001). Dapsone activation of CYP2C9-mediated metabolism: evidence for activation of multiple substrates and a two-site model. *Drug Metab. Dispos.* **29**, 1029–1034.
13. Tang, W. & Stearns, R. A. (2001). Heterotropic Cooperativity of Cytochrome P450 3A4 and Potential Drug–Drug Interactions. *Curr. Drug Metab.* **2**, 185–198.
14. Dabrowski, M. J., Schrag, M. L., Wienkers, L. C. & Atkins, W. M. (2002). Pyrene–pyrene complexes at the active site of cytochrome P450 3A4: evidence for a multiple substrate binding site. *J. Am. Chem. Soc.* **124**, 11866–11867.
15. Williams, P. A., Cosme, J., Ward, A., Angove, H. C., Matak Vinkovic, D. & Jhoti, H. (2003). Crystal structure of human cytochrome P450 2C9 with bound warfarin. *Nature*, **424**, 464–468.
16. Wester, M. R., Johnson, E. F., Marques-Soares, C., Dansette, P. M., Mansuy, D. & Stout, C. D. (2003). Structure of a substrate complex of mammalian

- cytochrome P450 2C5 at 2.3 Å resolution: evidence for multiple substrate binding modes. *Biochemistry*, **42**, 6370–6379.
17. Harris, D. & Loew, G. (1995). Prediction of regio-specific hydroxylation of camphor analogs by cytochrome P450cam. *J. Am. Chem. Soc.* **117**, 2738–2746.
 18. Das, B., Helms, V., Lounnas, V. & Wade, R. C. (2000). Multicopy molecular dynamics simulations suggest how to reconcile crystallographic and product formation data for camphor enantiomers bound to cytochrome P-450cam. *J. Inorg. Biochem.* **81**, 121–131.
 19. Omura, T. (1999). Forty years of cytochrome P450. *Biochem. Biophys. Res. Commun.* **266**, 690–698.
 20. Williams, P. A., Cosme, J., Sridhar, V., Johnson, E. F. & McRee, D. E. (2000). Mammalian microsomal cytochrome P450 monooxygenase: structural adaptations for membrane binding and functional diversity. *Mol. Cell*, **5**, 121–131.
 21. Scott, E. E., He, Y. A., Wester, M. R., White, M. R., Chin, C. C., Halpert, J. R. *et al.* (2003). An open conformation of mammalian cytochrome P450 2B4 at 1.6 Å resolution. *Proc. Natl Acad. Sci. USA*, **100**, 13196–13201.
 22. Hasemann, C. A., Kurumbail, R. G., Boddupalli, S. S., Peterson, J. A. & Deisenhofer, J. (1995). Structure and function of cytochromes P450: a comparative analysis of three crystal structures. *Structure*, **3**, 41–62.
 23. Poulos, T. L., Finzel, B. C. & Howard, A. J. (1986). Crystal structure of substrate-free *Pseudomonas putida* cytochrome P-450. *Biochemistry*, **25**, 5314–5322.
 24. Poulos, T. L., Finzel, B. C. & Howard, A. J. (1987). High resolution crystal structure of cytochrome P450cam. *J. Mol. Biol.* **195**, 687–700.
 25. Atkins, W. M. & Sligar, S. G. (1988). The roles of active site hydrogen bonding in cytochrome P-450cam as revealed by site-directed mutagenesis. *J. Biol. Chem.* **263**, 18842–18849.
 26. Atkins, W. M. & Sligar, S. G. (1989). Molecular recognition in cyt P450: alteration of regioselective alkane hydroxylation *via* protein engineering. *J. Am. Chem. Soc.* **111**, 2715.
 27. Raag, R. & Poulos, T. L. (1989). The structural basis for substrate-induced changes in redox potential and spin equilibrium in cytochrome P-450CAM. *Biochemistry*, **28**, 917–922.
 28. Raag, R. & Poulos, T. L. (1991). Crystal structures of cytochrome-P-450CAM complexed with camphane thiocamphor, and adamantane-factors controlling P-450 substrate hydroxylation. *Biochemistry*, **30**, 2674–2684.
 29. Raag, R., Li, H., Jones, B. C. & Poulos, T. L. (1993). Inhibitor-induced conformational change in cytochrome P-450CAM. *Biochemistry*, **32**, 4571–4578.
 30. Helms, V., Deprez, E., Gill, E., Barret, C., Hoa, G. H. B. & Wade, R. C. (1996). Improved binding of cytochrome P450cam substrate analogues designed to fill extra space in the substrate binding pocket. *Biochemistry*, **35**, 1485–1499.
 31. Sibbesen, O., Zhang, Z. & Ortiz de Montellano, P. R. (1998). Cytochrome P450cam substrate specificity: relationship between structure and catalytic oxidation of alkylbenzenes. *Arch. Biochem. Biophys.* **353**, 285–296.
 32. Jung, C. (2002). Cytochrome P-450-CO and substrates: lessons from ligand binding under high pressure. *Biochim. Biophys. Acta*, **1595**, 309–328.
 33. Wells, A. V., Li, P. S., Champion, P. M., Martinis, S. A. & Sligar, S. G. (1992). Resonance Raman investigations of *Escherichia coli*-expressed *Pseudomonas putida* cytochrome-P450 and cytochrome-P420. *Biochemistry*, **31**, 4384–4393.
 34. DiPrimo, C., Hoa, G. H. B., Deprez, E., Douzou, P. & Sligar, S. G. (1993). Conformational dynamics of cytochrome P450cam as monitored by photoacoustic calorimetry. *Biochemistry*, **32**, 3671–3676.
 35. Prasad, S. & Mitra, S. (2002). Role of protein and substrate dynamics in catalysis by *Pseudomonas putida* cytochrome P450cam. *Biochemistry*, **41**, 14499–14508.
 36. Ludemann, S. K., Lounnas, V. & Wade, R. C. (2000). How do substrates enter and products exit the buried active site of cytochrome P450cam? 2. Steered molecular dynamics and adiabatic mapping of substrate pathways. *J. Mol. Biol.* **303**, 813–830.
 37. Ludemann, S. K., Lounnas, V. & Wade, R. C. (2000). How do substrates enter and products exit the buried active site of cytochrome P450cam? 1. Random expulsion molecular dynamics investigation of ligand access channels and mechanisms. *J. Mol. Biol.* **303**, 797–811.
 38. Lounnas, V. & Wade, R. C. (1997). Exceptionally stable salt bridges in cytochrome P450cam have functional roles. *Biochemistry*, **36**, 5402–5417.
 39. Loida, P. J., Sligar, S. G., Paulsen, M. D., Arnold, G. E. & Ornstein, R. L. (1995). Stereoselective hydroxylation of norcamphor by cytochrome P450cam. *J. Biol. Chem.* **270**, 5326–5330.
 40. Podust, L. M., Poulos, T. L. & Waterman, M. R. (2001). Crystal structure of cytochrome P450 14 alpha-sterol demethylase (CYP51) from *Mycobacterium tuberculosis* in complex with azole inhibitors. *Proc. Natl Acad. Sci. USA*, **98**, 3068–3073.
 41. Podust, L., Kim, Y., Arase, M., Neely, B. A., Beck, B. J., Bach, H. *et al.* (2003). The 1.92 Å structure of *Streptomyces coelicolor* A3(2) CYP154C1: a new monooxygenase that functionalizes macrolide ring systems. *J. Biol. Chem.* **278**, 12214–12221.
 42. Wilker, J. J., Dmochowski, I. J., Dawson, J. H., Winkler, J. R. & Gray, H. B. (1999). Substrates for rapid delivery of electrons and holes to buried active sites in proteins. *Angewandte Chemie*, **38**, 90–92.
 43. Dmochowski, I. J., Crane, B. R., Wilker, J. J., Winkler, J. R. & Gray, H. B. (1999). Optical detection of cytochrome P450 by sensitizer-linked substrates. *Proc. Natl Acad. Sci. USA*, **96**, 12987–12990.
 44. Dunn, A. R., Dmochowski, I. J., Bilwes, A. M., Gray, H. B. & Crane, B. R. (2001). Probing the open state of cytochrome P450cam with ruthenium-linker substrates. *Proc. Natl Acad. Sci. USA*, **98**, 12420–12425.
 45. Dunn, A. R., Hays, A.-M.A., Goodin, D. B., Stout, C. D., Chiu, R., Winkler, J. R. & Gray, H. B. (2002). Fluorescent probes for cytochrome P450 structural characterization and inhibitor screening. *J. Am. Chem. Soc.* **124**, 10254–10255.
 46. Schlichting, I., Berendzen, J., Chu, K., Stock, A. M., Maves, S. A., Benson, D. E. *et al.* (2000). The catalytic pathway of cytochrome P450cam at atomic resolution. *Science*, **287**, 1615–1622.
 47. Raag, R., Martinis, S. A., Sligar, S. G. & Poulos, T. L. (1991). Crystal structure of the cytochrome-P-450CAM active site mutant Thr252Ala. *Biochemistry*, **30**, 11420–11429.
 48. Hayward, S. & Lee, R. A. (2002). Improvements in the analysis of domain motions in proteins from conformational change: DynDom version 1.50. *J. Mol. Graph. Model.* **21**, 181–183.

49. Hayward, S. (1999). Structural principles governing domain motions in proteins. *Proteins: Struct. Funct. Genet.* **36**, 425–435.
50. Raag, R. & Poulos, T. L. (1989). The structural basis for substrate induced changes in redox potential and spin equilibrium in P-450cam. *Biochemistry*, **28**, 917–922.
51. Fisher, M. T., Scarlata, S. F. & Sligar, S. G. (1985). High-pressure investigations of cytochrome P-450 spin and substrate binding equilibria. *Arch. Biochem. Biophys.* **240**, 456–463.
52. Di Gleria, K., Nickerson, D. P., Hill, H. A. O., Wong, L.-L. & Fulop, V. (1998). Covalent attachment of an electroactive sulfhydryl reagent in the active site of cytochrome P450cam as revealed by the crystal structure of the modified protein. *J. Am. Chem. Soc.* **120**, 46–52.
53. Gerstein, M. & Krebs, W. (1998). A database of macromolecular motions. *Nucleic Acids Res.* **26**, 4280–4290.
54. Teague, S. J. (2003). Implications of protein flexibility for drug discovery. *Nature Rev. Drug Discov.* **2**, 527–541.
55. Akamine, P., Madhusudan, Wu, J., Xuong, N. H., Ten Eyck, L. F. & Taylor, S. S. (2003). Dynamic features of cAMP-dependent protein kinase revealed by apo-enzyme crystal structure. *J. Mol. Biol.* **327**, 159–171.
56. Poulos, T. L. (1995). Cytochrome P450. *Curr. Opin. Struct. Biol.* **5**, 767–774.
57. Prasad, S., Mazumdar, S. & Mitra, S. (2000). Binding of camphor to *Pseudomonas putida* cytochrome P450cam: steady-state and picosecond time-resolved fluorescence studies. *FEBS Letters*, **477**, 157–160.
58. Peterson, J. A. & Graham-Lorence, S. E. (1995). Bacterial P450s: structural similarities and functional differences. In *Cytochrome P450: Structure, Mechanism and Biochemistry* (Ortiz de Montellano, P. R., ed.), 2nd edit., pp. 151–180, Plenum Press, New York.
59. Modi, S., Sutcliffe, M. J., Primrose, W. U., Lian, L. Y. & Roberts, G. C. (1996). The catalytic mechanism of cytochrome P450 BM3 involves a 6 Å movement of the bound substrate on reduction. *Nature Struct. Biol.* **3**, 414–417.
60. Li, H. & Poulos, T. L. (1997). The structure of the cytochrome p450BM-3 hemedomain complexed with the fatty acid substrate, palmitoleic acid. *Nature Struct. Biol.* **4**, 140–146.
61. Yano, J. K., Koo, L. S., Schuller, D. J., Li, H., De Montellano, P. R. O. & Poulos, T. L. (2000). Crystal structure of a thermophilic cytochrome P450 from the archaeon *Sulfolobus solfataricus*. *J. Biol. Chem.* **275**, 31086–31092.
62. Scott, E. E., White, M. A., He, Y. A., Johnson, E. F., Stout, C. D. & Halpert, J. R. (2004). Structure of mammalian cytochrome P450 2B4 complexed with 4-4-chlorophenyl imidazole at 1.9 Å resolution: insight into the range of P450 conformations and coordination of redox partner binding. *J. Biol. Chem.* **279**, 27294–27301.
63. Haines, D. C., Tomchick, D. R., Machius, M. & Peterson, J. A. (2001). Pivotal role of water in the mechanism of P450BM-3. *Biochemistry*, **40**, 13456–13465.
64. Tosha, T., Yoshioka, S., Takahashi, S., Ishimori, K., Shimada, H. & Morishima, I. (2003). NMR study on the structural changes of cytochrome P450cam upon the complex formation with putidaredoxin. *J. Biol. Chem.* **278**, 39809–39821.
65. Koellner, G., Kryger, G., Millard, C. B., Siman, I., Sussman, J. L. & Steiner, T. (2000). Active-site gorge and buried water molecules in crystal structures of acetylcholinesterase from *Tropedo californica*. *J. Mol. Biol.* **296**, 713–726.
66. Diprimo, C., Sligar, S. G., Hoa, G. H. B. & Douzou, P. (1992). A critical role of protein-bound water in the catalytic cycle of cytochrome-P-450 camphor. *FEBS Letters*, **312**, 252–254.
67. Tezcan, F. A., Winkler, J. R. & Gray, H. B. (1998). Effects of ligation and folding on reduction potentials of heme proteins. *J. Am. Chem. Soc.* **120**, 13383–13388.
68. Otwinowski, Z. & Minor, W. (1997). Processing of X-ray diffraction data collected in oscillation mode. *Methods Enzymol.* **276**, 307–326.
69. Brunger, A. T., Adams, P. D., Clore, G. M., DeLano, W. L., Gros, P., Grosse-Kunstleve, R. W. *et al.* (1998). Crystallography and NMR system: a new software suite for macromolecular structure determination. *Acta Crystallog. sect. D*, **54**, 905–921.
70. McRee, D. E. (1999). XtalView Xfit-A versatile program for manipulating atomic coordinates and electron density. *J. Struct. Biol.* **125**, 156–165.
71. Sheldrick, G. M. (1996). Least-squares refinement of macromolecules: estimated standard deviations, NCS restraints and factors affecting convergence. In *Proceedings of the CCP4 Study Weekend, January 1996* (Dodson, E., Moore, M., Ralph, A. & Bailey, S., eds), pp. 47–58, Daresbury Laboratory, Warrington, UK.
72. Laskowski, R. A., Moss, D. S. & Thornton, J. M. (1993). Main-chain bond lengths and bond angles in protein structures. *J. Mol. Biol.* **231**, 1049–1067.
73. Carson, M. (1997). Ribbons. *Methods Enzymol.* **277**, 493–505.

Edited by R. Huber

(Received 14 June 2004; received in revised form 17 September 2004; accepted 20 September 2004)